European Polymer Journal 158 (2021) 110652

Contents lists available at ScienceDirect

European Polymer Journal

journal homepage: www.elsevier.com/locate/europolj

User-friendly chemical patterning with digital light projection polymer brush photolithography

Michele Fromel [a], Raymond L. Crisci III [a], Chinmay S. Sankhe [a], Danielle Reifsnyder Hickey [c], Timothy B. Tighe [d], Esther W. Gomez [a,e], Christian W. Pester [a,b,c,*]

[a] Department of Chemical Engineering, The Pennsylvania State University, University Park, PA 16802, United States
[b] Department of Chemistry, The Pennsylvania State University, University Park, PA 16802, United States
[c] Department of Materials Science and Engineering, The Pennsylvania State University, University Park, PA 16802, United States
[d] Materials Research Institute, The Pennsylvania State University, University Park, PA 16802, United States
[e] Department of Biomedical Engineering, The Pennsylvania State University, University Park, PA 16802, United States

ARTICLE INFO

Keywords:
Photolithography
Polymer brushes
Surface
Photopolymerization
Controlled radical polymerization
Reversible addition fragmentation chain-transfer polymerization (RAFT)

ABSTRACT

Patterned polymeric coatings are broadly relevant for all areas of bioengineering: anti-biofouling, controlled protein adsorption, guided cell growth, and many more. This contribution describes a robust topographical and chemical patterning platform that combines an LED digital light projector with oxygen-tolerant light-mediated polymerization to design advanced surfaces on the micron scale and in mild ambient conditions. The user-friendly nature of this approach is targeted towards bringing complex chemical patterning abilities based on surface-tethered polymers into the hands of non-experts and enabling both fundamental and applied studies related to patterned surfaces in bioengineering.

1. Introduction

Chemical surface patterning with polymers allows for the fabrication of advanced and multi-functional coatings that are relevant for a plethora of applications: organic light-emitting diode displays [1], microfluidic devices [2], and flame-retardant coatings [3–9]. Examples for biological and biomedical applications include anti-biofouling [10], protein adsorption [11,12], the study of DNA [11–13], directed neuron [14] and cell growth [15,16], and the preparation of biomedical devices [17].

To address patterning limitations and other drawbacks of physisorbed coatings (e.g., delamination and leaching) [18], the covalent attachment of polymers has emerged as a viable strategy. Approaches towards such polymer brush surfaces include grafting polymers to, or growing them from a surface via surface-initiated (SI) polymerization [8,19]. Generally, the *patterning* of polymer brushes can be completed using either a "bottom-up" [10,12,20–23] or a "top-down" [24,25] approach. The former involves *pre-patterning of initiator monolayers* and subsequent amplification using SI polymerization. We refer the reader to excellent reviews [9,26–29] that describe related techniques, including microcontact printing (μCP) [27,30,31], ink-jet printing [27], e-beam lithography [28], laser-based lithography [27], scanning probe lithography [27], UV lithography [9,28], interference lithography [9], and dip-pen nanolithography [9].

In recent years, *externally regulated* SI polymerizations have emerged as mild and potent alternatives for the direct patterning of surfaces using polymer brushes [4–37]. Popular approaches include free-radical (SI-FRP) [32–34] and reversible deactivation radical polymerizations (SI-RDRPs), including nitroxide mediated (SI-NMP) [35], atom transfer radical (SI-ATRP) [36–38], and reversible addition-fragmentation chain transfer (SI-RAFT) polymerization [39]. Light in particular has been identified as an attractive external stimulus [40,41] that affords spatiotemporal control from uniform initiating layers through the use of binary or gradient photomasks [10,42]. With improved oxygen tolerance, an increasingly broad monomer scope, and the ability to topographically and chemically pattern surfaces with little effort, polymer brush photolithography is now on the verge of industrial adoption.

The use of photomasks for polymer brush patterning [38,43–47] is compatible with most photoredox chemistries, and allows for reliable reproduction of features with micron resolution. However, the need to

* Corresponding author at: Department of Chemical Engineering, Department of Chemistry, Department of Materials Science and Engineering, The Pennsylvania State University, United States.
E-mail address: pester@psu.edu (C.W. Pester).

https://doi.org/10.1016/j.eurpolymj.2021.110652
Received 16 April 2021; Received in revised form 9 July 2021; Accepted 15 July 2021
Available online 19 July 2021

manufacture an individual photomask for every desired pattern is expensive, time-intensive [48], and limited to flat substrates to assure good contact with the mask. This intimate contact with the reactants requires the photomask itself to be chemically resistant. Accidental movement of the photomask during polymerization can result in blurred images, and direct contact between the photomask and reaction solution can cause unwanted sticking to the substrate – especially during polymerization [47]. Finally, multi-step photomask patterning, requiring *in-situ* switching of photomasks, can result in misaligned reproduction of features.

Alternatives to conventional photomasks include inkjet-printed photomasks [43,49] and digital projection by digital micromirror devices (DMDs) or liquid crystal display (LCD) projectors, all of which have been used for the patterning of polymer brushes [50–53]. While effective, inkjet-printed mask approaches cannot be digitally modified, DMDs are costly, and LCD projectors feature ubiquitous white backlight which can lead to small amounts of polymer growth in regions not intentionally being patterned.

In this contribution, we describe a robust *light emitting diode (LED) digital light projector* (DLP)-based advanced manufacturing platform for *push-of-a-button surface patterning*. Leveraging recent advances in light-mediated, surface-initiated polymerization, this approach addresses the above limitations for surface patterning and combines the benefits of (i) digital projection and (ii) reduction lithography with (iii) the ability to perform multiple reactions both sequentially and simultaneously. The high contrast of the LED light source eliminates backlighting while providing a cost-effective approach to maintaining the simplicity of *in-situ* pattern modification and projection by external computer control. As an outcome, this provides a continuous time- and cost-efficient platform for advanced manufacturing of horizontally and vertically patterned surfaces with micron-scale resolution and significant chemical versatility.

2. Results and discussion

The LED DLP approach engineered in this work, consisting of the projector itself and an array of lenses that affords size-reduced projection of light onto a functionalized substrate for photoredox chemistry at the surface, is illustrated in Fig. 1a. A computer-generated image can be projected and reproduced in the form of a topographical polymer brush feature on a silicon substrate (see Fig. 1b). Furthermore, the use of oxygen-tolerant polymerization and a simple substrate stage provides opportunities for rapid and facile micron-scale chemical patterning of surfaces. The substrate is placed on a stainless-steel platform and pressed up against three pins, with heights shorter than the thickness of a typical silicon wafer ($d(SiO_2) = 500$ mm, Fig. 1c). A Pac-man shaped magnet is then used to fixate the substrate securely in place against the pins. The magnet, though not essential for single component patterning, is instrumental when patterning multiple components on the same surface. By holding the substrate securely in place against the raised pins, the magnet allows intermediate steps to be performed without disruption of the substrate position. This includes coverslip removal, surface rinsing and drying, deposition of new polymerization solution, and addition of a new coverslip. As such, high-resolution patterning of multiple components on a single surface is facilitated (see Fig. 4). Given the mobility of the magnetic anchor, this mechanism provides broad versatility with respect to substrate size and shape. Subsequently, the surface can be coated with reactant solution, covered with a coverslip to guarantee uniform spreading, and irradiated using the LED DLP (1080p resolution, 10,000:1 contrast ratio, 7500 lx).

Fig. 2b shows a representative optical micrograph of resulting micron-scale patterned polymer brushes. *N,N*-dimethylacrylamide (DMA) was polymerized using surface-initiated photoinduced electron transfer-reversible addition–fragmentation chain transfer polymerization (SI-PET-RAFT) [43] from SiO_2 substrates that were previously functionalized with 2-(dodecylthiocarbonothioylthio)-2-methyl-propanoic acid (DDMAT) chain transfer agents (CTAs). Using 5,10,15,20-tetraphenyl-21H,23H-porphine zinc (ZnTPP) as a photoredox catalyst (PC), polymerizations were performed at molar ratios of [Monomer]:[CTA]:[PC] = 500:1:0.025. Optical contrast results from distinct heights of the p(DMA) polymer brushes in separate areas as a result of different levels of photon flux, i.e., light intensity, from the LED projector. As evident from the optical and atomic force micrographs, no polymer growth was observed in the dark. In contrast to LCD projectors, LED DLPs provide improved contrast (10000:1, *"true black"*) that eliminates possible patterning limitations introduced by ubiquitous LCD backlighting. Atomic force microscopy (AFM) was used to verify topographical patterning (see Fig. 2c) with brightness of regions within the patterned film directly related to the polymer brush thickness. X-ray photoelectron spectroscopy (XPS) was used to verify the chemical fingerprint of p(DMA): C1s, O1s, and N1s peaks were observed at binding energies $BE_{C1s} = 285$, $BE_{O1s} = 532$ eV, and $BE_{N1s} = 400$ eV,

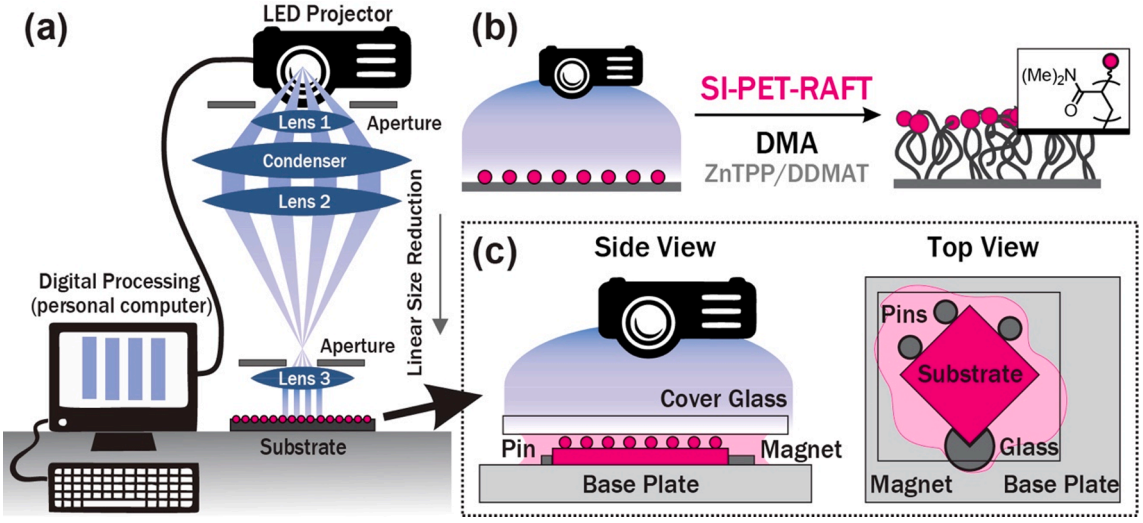

Fig. 1. (a) Schematic setup of LED digital light projection (DLP) of a computer-generated image onto a functionalized substrate for spatiotemporally controlled photochemistry. (b) Schematic of light-mediated polymerization of *N,N*-dimethylacrylamide (DMA) polymer brushes from a DDMAT functionalized substrate using a ZnTPP photoredox catalyst. (c) Side and top view of the substrate holder: three pins and a magnet are used to fix the substrate in place before it is covered by polymerization solution and a glass coverslip.

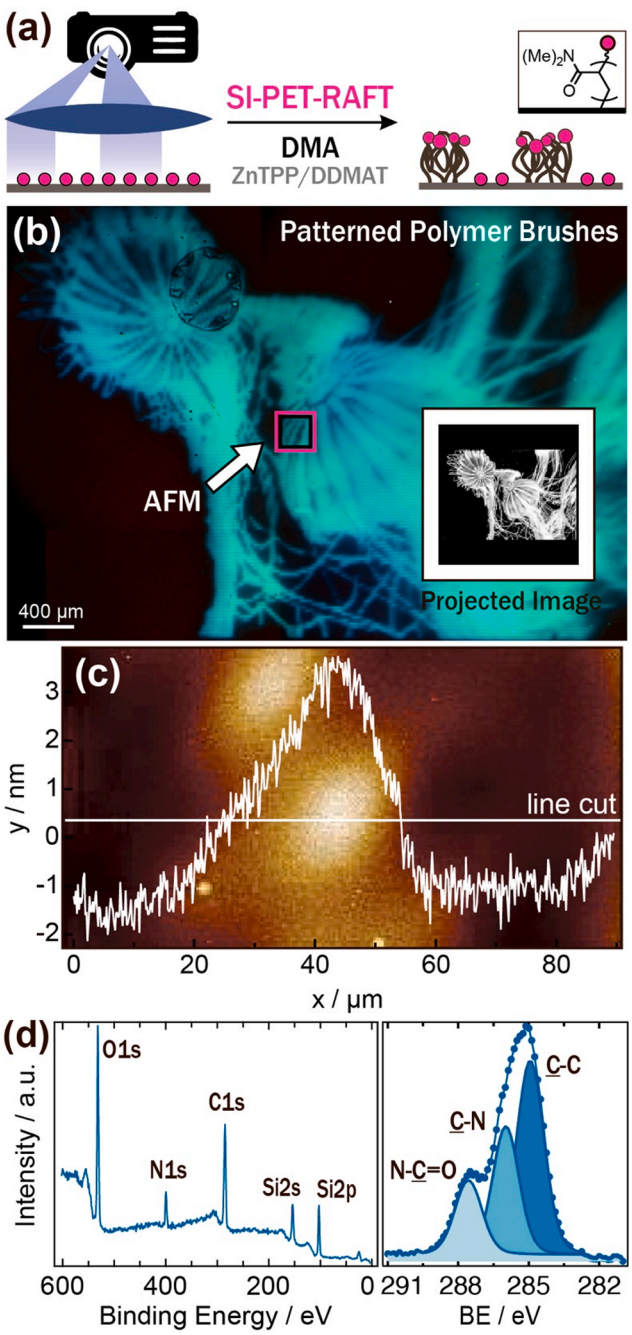

Fig. 2. (a) Schematic of chemical surface patterning using p(DMA) and LED DLP, (b) micrograph of p(DMA) brush pattern of original jellyfish photograph (inset) using the projector setup, and (c) atomic force micrograph of a portion of the patterned region boxed in pink in (b) showing the variation in polymer brush thickness across the area. (d) X-ray photoelectron survey and high-resolution carbon C1s spectra of the resulting pattern.

respectively (see Fig. 2d). The measured ratio of carbon to nitrogen from the XPS survey scan (C:N ≅ 5.0) also closely matches the theoretical value of C:N = 4.3 based on the molecular repeat unit, with the carbon % elevation likely due to minor organic surface contaminations. Silica Si2s and Si2p peaks result from the underlying substrate and are to be expected: the probing X-ray footprint exceeds the size of the pattern features. The high-resolution carbon C1s scan provides additional support for the presence of p(DMA), showing three distinct components matching the three major carbon environments: the amide carbonyl (Me_2N—(C═O)), —C—N—(C═O), and aliphatic C—C bonds. Significantly, this process is fully oxygen-tolerant (vide infra) and allows for polymer brush patterning without prior degassing and in ambient environment and temperatures.

The experimental setup consists of an LED projector with an internal lens of focal length $f_{proj.} = 190$ mm, followed by an array of four lenses: $f_1 = 100$ mm, $f_{cond.} = 60$ mm (condenser lens), $f_2 = 500$ mm, and $f_3 = 100$ mm. At a native resolution of 1920 × 1080 px^2, one pixel on the computer screen is reproduced at a size of approximately 25 μm^2 on the substrate, with the individual pixels visible in the projected pattern (see Fig. 2b). The obtainable resolution of this setup is diffraction-limited and hypothetically affords patterns on the order of half the wavelength of light that is used for photoredox catalysis. As such, improved optics and focusing is anticipated to provide sub-micron features (approximately $d = \lambda_{max}/2 \sim 210$ nm with λ_{max}(ZnTPP) = 425 nm) [54]. The impact of diffusion on resolution is negligible due to the short excited state lifetimes of common PCs (e.g., τ(ZnTPP) = 2.3 ps [55,56], τ(Ir(ppy)$_3$) = 50 ns) [22]. With diffusion constants of the PC species on the nanoscale per second (e.g., $D = 2.3 \times 10^{-9} m^2\ s^{-1}$ for Ir(ppy)$_3$) [22], excited state PC diffusion is limited to a few nanometers. Consequently, PC diffusion from the projected beam path into dark areas is not anticipated to adversely influence pattern resolution.

Previous studies on O_2-tolerant polymer brush photolithography approaches [57–59] often describe edge effects. Limited patterning capabilities at the outer boundaries of projected patterns and related artifacts (edge effects) are related to O_2 permeation. Oxidation of the PC (rendering it ineffective) [57] and decreasing efficacy of RDRP in the presence of O_2 are two possible contributing factors that are both inherently more pronounced at the edges of the projected patterns [58,59].

The described LED DLP platform can be used to avoid such edge artifacts by creating an effective photocatalytic "oxygen barrier" (see Fig. 3). The chemistry employed in these patterning experiments consists of a stock solution of ZnTPP photocatalyst dissolved in DMSO, which is added to a mixture of monomer and free RAFT CTA to make the complete polymerization solution [43]. The use of DMSO is essential to allow for oxygen tolerance through the PET-RAFT mechanism [60], wherein the unique interaction between ZnTPP and DMSO establishes oxygen-tolerance. Upon irradiation, ZnTPP rapidly converts $^3O_2$ (triplet oxygen) to $^1O_2$ (singlet oxygen) that is chemically quenched by the solvent, dimethyl sulfoxide (DMSO), to form dimethyl sulfone ($DMSO_2$) [60]. By projecting a white border around the desired pattern (see Fig. 3b, inset), this chemical transformation can be leveraged to introduce an oxygen barrier to "protect" the main patterning area. Using this approach, reactive oxygen species that are diffusing into the solution (from the edges and between the substrate and coverslip) are therefore removed and cannot have adverse effects on the SI-PET-RAFT equilibrium and performance. The resulting optical micrograph (see Fig. 3b) represents the entirety of the desired pattern without any edge artifacts. In comparison, Fig. 3c shows the result of a patterning attempt *without* this "white frame" oxygen barrier: the optical micrograph clearly shows significant patterning errors at the edges of the projected image (shown in the inset).

For more complex surface engineering, this approach allows for multicomponent patterning in a user-friendly manner and in ambient atmosphere. After an initial polymerization is completed, the glass coverslip can be removed, the surface rinsed and dried with a stream of air/nitrogen, and subsequently covered with another (same or different) polymerization solution without moving the substrate during the process. Recently, the concept of stop-flow chemistry was introduced to perform micron-scale patterning using light-mediated SI-ATRP [49]. While this work also allowed the continuous exchange of reactants, limitations remained regarding oxygen tolerance (sparging was required), and the use of inkjet-printed masks, while cost-effective, was limiting in the ability to perform sequential reactions in close vicinity on the surface without edge artifacts. Here, these limitations are circumvented by leveraging the oxygen tolerance of SI-PET-RAFT. Combining

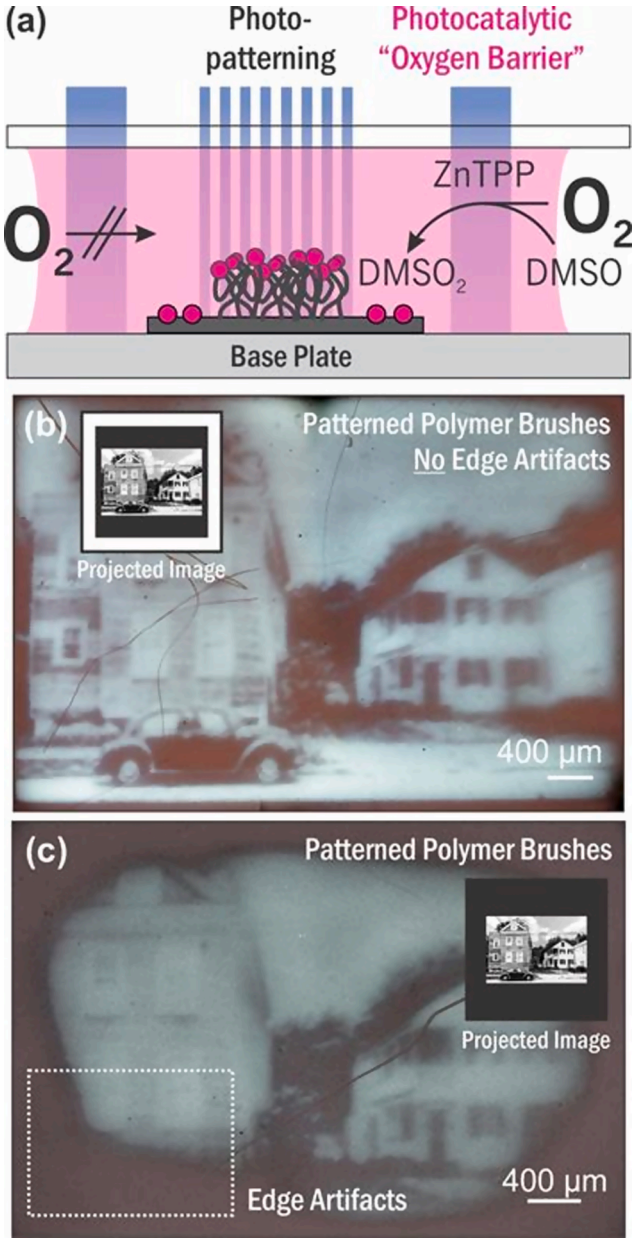

Fig. 3. (a) Reactive oxygen species can be photocatalytically quenched (converting DMSO to $DMSO_2$) at the far edges of the projection area to prevent artifacts. The resulting optical micrographs of p(DMA) patterns: (b) with and (c) without projection of a protective outer white border as an effective "oxygen-barrier," resulting in (b) complete and (c) incomplete image reproduction, respectively.

the advantages of the SI-PET-RAFT technique and the projector setup, a multicomponent pattern consisting of a poly(ethylene glycol) methyl ether methacrylate (PEGMA)/pentafluorophenyl methacrylate (PFPMA) copolymer, p(PEGMA-*co*-PFPMA), and p(DMA) in separate regions was prepared (see Fig. 4) on an SiO_2 substrate functionalized with 4-Cyano-4-[(dodecylsulfanylthiocarbonyl)sulfanyl]pentanoic acid (CDTPA) CTAs. A photograph of a city street was edited digitally to isolate the street lines, which were first polymerized using a 80:20 mixture by mol. % of PEGMA:PFPMA in a total solution ratio of [Monomer]:[CTA]:[PC] = 500:1:0.1. Following patterning of these copolymer brushes in the street line region and subsequent surface cleaning, the remaining features of the image were projected and patterned in p(DMA) brushes using a solution of [Monomer]:[CTA]:[PC] = 500:1:0.025 to give the final, complete multicomponent pattern (see Fig. 4c). Despite the low signal in scanning electron microscopy, energy dispersive X-ray spectroscopy (EDX) was used to verify the presence of nitrogen from p(DMA) and fluorine from p(PEGMA-*co*-PFPMA) in alternating street lines (see Fig. 4d). Despite the weak signal in the F K series due to only 20% incorporation of PFPMA in the copolymer, the overlay of the N K series and F K series highlights distinctive regions of p(DMA) and p(PEGMA-*co*-PFPMA). Additional support for the p(PEGMA-*co*-PFPMA) copolymer region is provided by analysis of the O K series, since the PEGMA component of the copolymer contributes significant oxygen to the region. A higher photocatalyst concentration was utilized in the case of the methacrylic copolymer growth to compensate for the slower methacrylate polymerization. The additional photocatalyst served to increase radical concentration and accelerate polymerization [61]. The use of PFPMA as a co-monomer also allows the possibility for post-functionalization of the patterned polymer brushes. As demonstrated in Fig. 4e, an amine-containing fluorescent dye (Alexa Fluor 488) was able to be selectively attached to polymer brushes in the p(PFPMA)-containing regions. This further highlights the advantages of this system to allow not only selective patterning of polymer materials but also the potential to selectively post-modify specific regions after initial patterning is completed.

3. Conclusions and outlook

The described LED DLP setup provides a user-friendly and robust platform for complex topographical and chemical patterning. Leveraging oxygen-tolerant surface-initiated polymerization techniques in a sequential manner on a fixed substrate provides a facile approach to exchanging chemistries *in-situ* to afford complex micron-scale patterning. This work highlights the benefits of digital image processing (e.g. addition of a white border to eliminate edge effects) on the precise reproduction of desired patterns using polymer brush photolithography. Further, it demonstrates the ability to combine polymer species of various functionalities on a single surface, opening the door to advanced material production and post-modification. Future work will include expansion to substrates of larger sizes and of different morphologies. With only slight modifications, e.g., the use of translational stages and additional digital image processing, such patterning can be made accessible.

Further, we will target high-resolution, multicomponent sequential patterning that leverages LED DLP projection as a variable wavelength light source. This is anticipated to allow for wavelength orthogonal reactions to move beyond many of the current methods for fabrication of patterned and mixed brush surfaces. In addition, we aim to employ this photolithography method for the patterning of additional classes of polymers both individually and in combination to impart surface properties relevant to various biological applications. An initial target will be multicomponent patterning of poly(ethylene glycol) methyl ether methacrylate and 2,2,2-trifluoroethyl methacrylate, a combination of species that we have previously demonstrated to be effective as an anti-biofouling coating [10]. Finally, we intend to expand to additional oxygen-tolerant polymerization systems, targeting aqueous polymerizations as a further improvement in not only the user-friendliness but also the eco-friendliness of this system.

4. Materials and methods

4.1. General material information

N,N-dimethylacrylamide (DMA), poly(ethylene glycol) methyl ether methacrylate (PEGMA), pentafluorophenol, methacryloyl chloride, triethylamine, 2-(dodecylthiocarbonothioylthio)-2-methylpropionic acid (DDMAT), cyano-4-[(dodecylsulfanylthiocarbonyl)sulfanyl] pentanoic acid (CDTPA), 5,10,15,20-Tetraphenyl-21*H*,23*H*-porphine zinc (ZnTPP), (3-aminopropyl)triethoxysilane (APTES), N-(3-dimethylaminopropyl)-N'-ethylcarbodiimide hydrochloride (EDC HCl), sodium

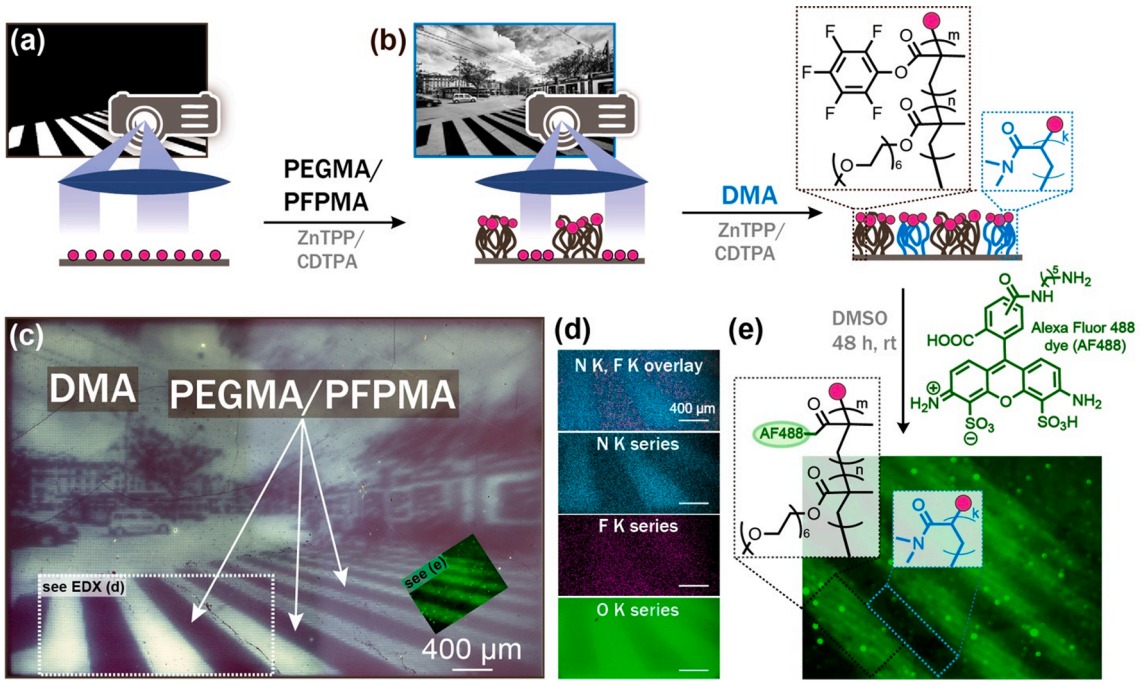

Fig. 4. Multicomponent patterning of first (a) street lines in p(PEGMA-*co*-PFPMA) (80:20 PEGMA:PFPMA by mol %) followed by (b) remaining features in p(DMA) brushes to give a final, multicomponent pattern (c) characterized by (d) EDX, highlighting the presence of nitrogen and fluorine in the boxed p(DMA) and p(PEGMA-*co*-PFPMA) regions in (c), respectively. An overlay of the N K (blue) and F K (purple) series highlights the contrast between the two individual channels shown below. The O K series further supports the more oxygen-dense p(PEGMA-*co*-PFPMA) regions. (e) Post-functionalization of p(PFPMA) brushes with Alexa Fluor 488 fluorescent dye characterized by fluorescence microscopy for the region overlayed in (c).

bicarbonate, magnesium sulfate, tetrahydrofuran (THF), dimethyl sulfoxide (DMSO), and ethyl acetate were purchased from Sigma-Aldrich and used as received (unless otherwise noted). Dichloromethane (DCM), toluene, isopropyl alcohol, acetone, and hexanes were purchased from Fisher Scientific and used as received. Alexa Fluor 488 cadaverine dye was purchased from Thermo Fisher and used as received. Silicon wafers with a 100 nm thermal oxide layer were purchased from WaferPro, LLC (San Jose, CA). A WiMiUS S1 Native 1080p LED projector was purchased from Amazon, and all other lenses and apertures utilized in the setup were purchased from Thorlabs.

4.2. Surface characterization

Nuclear magnetic resonance (NMR) spectra were recorded using a Bruker AVIII-HD-500 MHz instrument. All ^{1}H NMR experiments are reported in δ units, parts per million (ppm), and were normalized to the signal for the deuterated solvent $CDCl_3$ (7.26 ppm). X-ray photoelectron spectroscopy (XPS) measurements were performed using a Physical Electronics PHI VersaProbe II Spectrometer with a monochromatic Aluminum Kα X-ray source (1486.6 eV) under a vacuum of 10^{-8} Torr. Spectra were analyzed using CasaXPS software (Casa Software Ltd.). Atomic Force Microscopy (AFM) was performed using a Bruker BioScope Resolve Bio-AFM using ScanAsyst® mode. The measurement was conducted using a silicon nitride cantilever with a silicon tip. Scanning electron microscopy, energy dispersive X-ray spectroscopy (SEM-EDX) was performed using a Thermo Fisher Scientific Apreo S SEM. Optical micrographs of polymer brush patterns were captured using a Carl Zeiss Axio Scope A1 equipped with an Axiocam 305 color camera. Fluorescence micrographs were captured using a 10× air objective on a Nikon Eclipse Ti-E inverted fluorescence microscope equipped with a Photometrics CoolSNAP HQ^2 CCD camera.

4.3. Synthesis of DDMAT and CDTPA surface initiators

DDMAT and CDTPA surface initiators were synthesized according to established procedures [43], and characterized via ^{1}H NMR spectroscopy. DDMAT surface initiator: ^{1}H NMR (500 MHz, $CDCl_3$, 25 °C, *δ*, ppm): 0.61 (t, 2H), 0.90 (t, 3H), 1.24 (t, 9H), 1.30 (m, 18H), 1.59 (m, 2H), 1.65 (m, 2H), 1.71 (s, 6H), 3.22 (q, 2H), 3.26 (t, 2H), 3.82 (q, 6H), 6.65 (t, 1H); CDTPA surface initiator: ^{1}H NMR (500 MHz, $CDCl_3$, 25 °C, *δ*, ppm): 0.66 (t, 2H), 0.90 (t, 3H), 1.26 (t, 9H), 1.32 (m, 18H), 1.41 (m, 2H), 1.69 (m, 4H), 1.91 (s, 3H), 2.40 (m, 1H), 2.50 (m, 3H), 3.28 (q, 2H), 3.35 (t, 2H), 3.75 (q, 1H), 3.85 (q, 5H), 7.28 (s, 1H).

4.4. Surface-functionalization

Silicon wafers were broken into pieces of ~1 cm × 1 cm and sonicated for 10 min in toluene followed by 10 min in isopropyl alcohol to remove any pre-existing residues. Substrates were then dried with a stream of nitrogen and arranged in a petri dish, avoiding overlap. In the uncovered petri dish, substrates were treated with an air plasma cleaner (PDC-001, Harrick Plasma) under 300 mTorr vacuum for 10 min. During this time, a dilute (0.05% v/v) solution of DDMAT or CDTPA surface initiator (20 µL) in dry toluene (40 mL) was prepared. This solution was distributed into two 24 mL syringes and, promptly after removing substrates from the plasma cleaner, pushed into the petri dish through syringe filters. The petri dish was then covered and allowed to sit for ~48 h at room temperature, after which time the substrates were rinsed with toluene followed by isopropyl alcohol and dried under a stream of nitrogen. To maintain surface initiator integrity, substrates were stored in an inert nitrogen glovebox prior to use [62].

4.5. General method of surface-initiated photopatterning using projector

Stock solutions containing 1 mg of photocatalyst (ZnTPP) in 1 mL DMSO and 2 mg of photocatalyst (ZnTPP) in 1 mL DMSO were prepared in vials and stored in the dark. Monomers that contained inhibitor upon purchase were purified through a basic alumina column to remove the inhibitor prior to use. The inhibitor-free monomers, RAFT CTA, and ZnTPP/DMSO stock solution were mixed with a molar ratio of

[Monomer]:[CTA]:[ZnTPP] = 500:1:0.025 (DMA, 1 mg/mL ZnTPP/DMSO stock solution) or 500:1:0.1 (80:20 PEGMA/PFPMA, 2 mg/mL ZnTPP/DMSO stock solution) to form the reaction mixture. A CTA-functionalized thermal oxide silicon wafer was placed on top of the projector platform and secured in place by pressing up against the three raised pins with the Pac-man magnet applying pressure from the final corner. The reaction mixture was then dropped onto the wafer until completely covered. A glass coverslip was placed on top of the wafer to form a thin layer of solution in between the coverslip and wafer. The sample was then irradiated with a black and white pattern displayed from a computer attached via HDMI. The wafer was irradiated for the desired amount of time, then removed from the wafer platform and thoroughly rinsed with toluene, DCM, and isopropyl alcohol, then dried under a nitrogen stream. Final patterned surfaces were imaged by optical microscopy.

4.6. Synthesis of pentafluorophenyl methacrylate (PFPMA) monomer

A 100 mL round-bottom flask was charged with pentafluorophenol (5.83 g, 0.032 mol) and triethylamine (6.5 mL, 0.047 mol) in 25 mL of tetrahydrofuran (THF) and began to stir. The flask was placed in an ice bath at 0 °C. Methacryloyl chloride (MAC) (3 mL, 0.031 mol) was then added dropwise to the stirring reaction mixture. The reaction was stirred for 24 h at room temperature. After 24 h, the reaction mixture had changed from white to yellow and was concentrated in vacuo. The excess MAC was removed by dissolution in dichloromethane and was washed with deionized water, followed by saturated sodium bicarbonate solution, and finally deionized water. The pure organic layer was dried over magnesium sulfate salts, filtered, and concentrated in vacuo to give a yellow liquid product. ^{1}H NMR (500 MHz, $CDCl_3$, 25 °C, δ, ppm): 2.11 (s, 3H), 5.93 (s, 1H), 6.47 (s, 1H).

4.7. Multicomponent patterning

All procedures for general patterning were followed for the first polymerization. After the first component was patterned, the projector was turned off, and the coverslip was carefully removed from the silicon wafer. The wafer was kept in place by the pins and Pac-man magnet of the wafer platform. The surface of the wafer was then thoroughly rinsed with various solvents including DCM, toluene, deionized water, acetone, and isopropyl alcohol, then dried with a stream of air. This process was repeated until the wafer surface appeared to be free of any residual solution from the first polymerization step. Solution for the second polymerization step was then dropped onto the wafer and again covered with a coverslip. The second desired pattern was then projected onto the surface for the desired amount of time and ultimately rinsed with DCM, toluene, and isopropyl alcohol, then dried under a stream of nitrogen.

4.8. Pentafluorophenyl methacrylate polymer brush post-modification

In a 20 mL vial, approximately 0.2 mg of Alexa Fluor 488 cadaverine dye was dissolved in 2 mL of DMSO to give a fluorescent green solution. A wafer containing p(PFPMA) brushes was submerged in the solution until it was fully covered, with the reacting side facing upward. The vial was wrapped in aluminum foil, and the wafer was soaked for 48 h. Once removed from solution, the wafer was thoroughly rinsed with deionized water followed by isopropyl alcohol and stored in the dark until analyzed.

Declaration of Competing Interest

The authors declare that they have no known competing financial interests or personal relationships that could have appeared to influence the work reported in this paper.

Acknowledgements

This work was supported by start-up funds generously provided by the Pennsylvania State University. D. R. S. acknowledges funding from the National Science Foundation (NSF) through the Pennsylvania State University 2D Crystal Consortium–Materials Innovation Platform (2DCC-MIP) under NSF cooperative agreement DMR-1539916. E. W. G. acknowledges funding from NSF CMMI-1751785. We would like to acknowledge Trevor Clark and Jeff Shallenberger from the Penn State Materials Characterization Lab for assistance with SEM and XPS measurements, respectively. We appreciate the help Ellis Dunklebarger for the designing and engineering of the wafer stage.

Data availability

The raw/processed data required to reproduce these findings cannot be shared at this time due to technical or time limitations.

References

[1] Z.A. Page, B. Narupai, C.W. Pester, R. Bou Zerdan, A. Sokolov, D.S. Laitar, S. Mukhopadhyay, S. Sprague, A.J. McGrath, J.W. Kramer, P. Trefonas, C. J. Hawker, Novel strategy for photopatterning emissive polymer brushes for organic light emitting diode applications, ACS Cent. Sci. 3 (6) (2017) 654–661, https://doi.org/10.1021/acscentsci.7b00165.
[2] A. Sidorenko, T. Krupenkin, A. Taylor, P. Fratzl, J. Aizenberg, Reversible switching of hydrogel-actuated nanostructures into complex micropatterns, Science 315 (5811) (2007) 487–490, https://doi.org/10.1126/science.1135516.
[3] S. Liang, N.M. Neisius, S. Gaan, Recent developments in flame retardant polymeric coatings, Prog. Org. Coatings 76 (11) (2013) 1642–1665, https://doi.org/10.1016/j.porgcoat.2013.07.014.
[4] C.F. Welch, R.P. Hjelm, J.T. Mang, M.E. Hawley, D.A. Wrobleski, E. Bruce Orler, J. B. Kortright, Resonant soft X-ray scattering and reflectivity study of the phase-separated structure of thin poly(styrene-b-methyl methacrylate) films, J. Polym. Sci. Part B Polym. Phys. 51 (2) (2013) 149–157, https://doi.org/10.1002/polb.23190.
[5] U. Schmelmer, A. Paul, A. Küller, M. Steenackers, A. Ulman, M. Grunze, A. Gölzhäuser, R. Jordan, Nanostructured polymer brushes, Small 3 (3) (2007) 459–465, https://doi.org/10.1002/(ISSN)1613-682910.1002/smll.v3:310.1002/smll.200600528.
[6] A. Olivier, F. Meyer, J.M. Raquez, P. Damman, P. Dubois, Surface-initiated controlled polymerization as a convenient method for designing functional polymer brushes: from self-assembled monolayers to patterned surfaces, Prog. Polym. Sci. 37 (1) (2012) 157–181, https://doi.org/10.1016/j.progpolymsci.2011.06.002.
[7] T. Wu, K. Efimenko, J. Genzer, Combinatorial study of the mushroom-to-brush crossover in surface anchored polyacrylamide, J. Am. Chem. Soc. 124 (32) (2002) 9394–9395, https://doi.org/10.1021/ja027412n.
[8] B. Li, B. Yu, Q. Ye, F. Zhou, Tapping the potential of polymer brushes through synthesis, Acc. Chem. Res. 48 (2) (2015) 229–237, https://doi.org/10.1021/ar500323p.
[9] T. Chen, I. Amin, R. Jordan, Patterned polymer brushes, Chem. Soc. Rev. 41 (8) (2012) 3280, https://doi.org/10.1039/c2cs15225h.
[10] C.W. Pester, J.E. Poelma, B. Narupai, S.N. Patel, G.M. Su, T.E. Mates, Y. Luo, C. K. Ober, C.J. Hawker, E.J. Kramer, Ambiguous anti-fouling surfaces: facile synthesis by light-mediated radical polymerization, J. Polym. Sci. Part A Polym. Chem. 54 (2) (2016) 253–262, https://doi.org/10.1002/pola.27748.
[11] S. Morgenthaler, C. Zink, N.D. Spencer, Surface-chemical and -morphological gradients, Soft Matter 4 (3) (2008) 419–434, https://doi.org/10.1039/b715466f.
[12] M. Kaholek, W.-K. Lee, B. LaMattina, K.C. Caster, S. Zauscher, Fabrication of stimulus-responsive nanopatterned polymer brushes by scanning-probe lithography, Nano Lett. 4 (2) (2004) 373–376, https://doi.org/10.1021/nl035054w10.1021/nl035054w.s001.
[13] H. Cao, J.O. Tegenfeldt, R.H. Austin, S.Y. Chou, Gradient nanostructures for interfacing microfluidics and nanofluidics, Appl. Phys. Lett. 81 (16) (2002) 3058–3060, https://doi.org/10.1063/1.1515115.
[14] Z. Zhou, P. Yu, H.M. Geller, C.K. Ober, Biomimetic polymer brushes containing tethered acetylcholine analogs for protein and hippocampal neuronal cell patterning, Biomacromolecules 14 (2) (2013) 529–537, https://doi.org/10.1021/bm301785b.
[15] B.L. Leigh, E. Cheng, L. Xu, C. Andresen, M.R. Hansen, C.A. Guymon, Photopolymerizable zwitterionic polymer patterns control cell adhesion and guide neural growth, Biomacromolecules 18 (8) (2017) 2389–2401, https://doi.org/10.1021/acs.biomac.7b0057910.1021/acs.biomac.7b00579.s001.
[16] X. Chen, H. Shang, S. Cao, H. Tan, J. Li, A zwitterionic surface with general cell-adhesive and protein-resistant properties, RSC Adv. 5 (93) (2015) 76216–76220, https://doi.org/10.1039/c5ra16883j.
[17] H. Murata, B.-J. Chang, O. Prucker, M. Dahm, J. Rühe, Polymeric coatings for biomedical devices, Surf. Sci. 570 (1–2) (2004) 111–118, https://doi.org/10.1016/j.susc.2004.06.185.

[18] K. Norrman, A. Ghanbari-Siahkali, N.B. Larsen, 6 studies of spin-coated polymer films, Annu. Rep. Prog. Chem., Sect. C: Phys. Chem. 101 (2005) 174, https://doi.org/10.1039/b408857n.

[19] J.O. Zoppe, N.C. Ataman, P. Mocny, J. Wang, J. Moraes, H.-A.-A. Klok, Surface-initiated controlled radical polymerization: state-of-the-art, opportunities, and challenges in surface and interface engineering with polymer brushes, Chem. Rev. 117 (3) (2017) 1105–1318, https://doi.org/10.1021/acs.chemrev.6b00314.

[20] R.D. Piner, J. Zhu, F. Xu, S. Hong, C.A. Mirkin, "Dip-Pen" nanolithography, Science 283 (1999) 661–663, https://doi.org/10.1126/science.283.5402.661.

[21] W. Eck, V. Stadler, W. Geyer, M. Zharnikov, A. Gölzhäuser, M. Grunze, Generation of surface amino groups on aromatic self-assembled monolayers by low energy electron beams - a first step towards chemical lithography, Adv. Mater. 12 (11) (2000) 805–808, https://doi.org/10.1002/(SICI)1521-4095(200006)12:11<805::AID-ADMA805>3.0.CO;2-0.

[22] J.E. Poelma, B.P. Fors, G.F. Meyers, J.W. Kramer, C.J. Hawker, Fabrication of complex three-dimensional polymer brush nanostructures through light-mediated living radical polymerization, Angew. Chemie Int. Ed. 52 (27) (2013) 6844–6848, https://doi.org/10.1002/anie.201301845.

[23] E.H. Discekici, C.W. Pester, N.J. Treat, J. Lawrence, K.M. Mattson, B. Narupai, E. P. Toumayan, Y. Luo, A.J. McGrath, P.G. Clark, J. Read de Alaniz, C.J. Hawker, Simple benchtop approach to polymer brush nanostructures using visible-light-mediated metal-free atom transfer radical polymerization, ACS Macro Lett. 5 (2) (2016) 258–262, https://doi.org/10.1021/acsmacrolett.6b0000410.1021/acsmacrolett.6b00004.s001.

[24] A. Rastogi, M.Y. Paik, M. Tanaka, C.K. Ober, Direct patterning of intrinsically electron beam sensitive polymer brushes, ACS Nano 4 (2) (2010) 771–780, https://doi.org/10.1021/nn901344u.

[25] S. Sun, M. Montague, K. Critchley, M.-S. Chen, W.J. Dressick, S.D. Evans, G. J. Leggett, Fabrication of biological nanostructures by scanning near-field photolithography of chloromethylphenylsiloxane monolayers, Nano Lett. 6 (1) (2006) 29–33, https://doi.org/10.1021/nl051804l.

[26] X. Lin, Q. He, J. Li, Complex polymer brush gradients based on nanolithography and surface-initiated polymerization, Chem. Soc. Rev. 41 (9) (2012) 3584, https://doi.org/10.1039/c2cs15316e.

[27] J.-K. Chen, C.-J. Chang, Fabrications and applications of stimulus-responsive polymer films and patterns on surfaces: a review, Materials. 7 (2) (2014) 805–875, https://doi.org/10.3390/ma7020805.

[28] M.E. Welch, C.K. Ober, Responsive and patterned polymer brushes, J. Polym. Sci., Part B: Polym. Phys. 51 (20) (2013) 1457–1472, https://doi.org/10.1002/polb.23356.

[29] R. Ducker, A. Garcia, J. Zhang, T. Chen, S. Zauscher, Polymeric and biomacromolecular brush nanostructures: progress in synthesis, patterning and characterization, Soft Matter. 4 (9) (2008) 1774, https://doi.org/10.1039/b804861b.

[30] M. Husemann, D. Mecerreyes, C.J.J. Hawker, J.L.L. Hedrick, R.R. Shah, N.L. L. Abbott, Surface-initiated polymerization for amplification of self-assembled monolayers patterned by microcontact printing, Angew. Chemie Int. Ed. 38 (5) (1999) 647–649, https://doi.org/10.1002/(sici)1521-3773(19990301)38:5<647::aid-anie647>3.0.co;2-0.

[31] S. Lamping, C. Buten, B.J. Ravoo, Functionalization and patterning of self-assembled monolayers and polymer brushes using microcontact chemistry, Acc. Chem. Res. 52 (2019) 1336–1346, https://doi.org/10.1021/acs.accounts.9b00041.

[32] G. Boven, M.L.C.M. Oosterling, G. Challa, A. Jan Schouten, Grafting kinetics of poly(methyl methacrylate) on microparticulate silica, Polymer (Guildf). 31 (12) (1990) 2377–2383, https://doi.org/10.1016/0032-3861(90)90327-U.

[33] O. Prucker, J. Ruehe, Grafting of polymers to solid surfaces by using immobilized azoinitiators, Mater. Res. Soc. Symp. Proc. 304 (1993) 167–172, https://doi.org/10.1557/proc-304-167.

[34] V.N. Fery, R. Laible, K. Hamann, Polyreaktionen an Pigmentoberflächen. III. Mitteilung: Polyreaktionen an SiO2-oberflächen, Die Angew. Makromol. Chemie 34 (1) (1973) 81–109, https://doi.org/10.1002/apmc.1973.050340107.

[35] Marc Husseman, Eva E. Malmström, Molly McNamara, Mathew Mate, David Mecerreyes, Didier G. Benoit, James L. Hedrick, Paul Mansky, E. Huang, Thomas P. Russell, Craig J. Hawker, Controlled synthesis of polymer brushes by "living" free radical polymerization techniques, Macromolecules 32 (5) (1999) 1424–1431, https://doi.org/10.1021/ma981290v.

[36] X. Huang, M.J. Wirth, Surface-initiated radical polymerization on porous silica, Anal. Chem. 69 (22) (1997) 4577–4580, https://doi.org/10.1021/ac9704523.

[37] M. Ejaz, S. Yamamoto, K. Ohno, Y. Tsujii, T. Fukuda, Controlled graft polymerization of methyl methacrylate on silicon substrate by the combined use of the langmuir-blodgett and atom transfer radical polymerization techniques, Macromolecules 31 (17) (1998) 5934–5936, https://doi.org/10.1021/ma980240n.

[38] B. Narupai, J.E. Poelma, C.W. Pester, A.J. McGrath, E.P. Toumayan, Y. Luo, J. W. Kramer, P.G. Clark, P.C. Ray, C.J. Hawker, Hierarchical comb brush architectures via sequential light-mediated controlled radical polymerizations, J. Polym. Sci. Part A Polym. Chem. 54 (15) (2016) 2276–2284, https://doi.org/10.1002/pola.28128.

[39] M. Baum, W.J.J. Brittain, Synthesis of polymer brushes on silicate substrates via reversible addition fragmentation chain transfer technique, Macromolecules 35 (3) (2002) 610–615, https://doi.org/10.1021/ma0112467.

[40] R.C. McAtee, E.J. McClain, C.R.J. Stephenson, Illuminating photoredox catalysis, Trends Chem. 1 (1) (2019) 111–125, https://doi.org/10.1016/j.trechm.2019.01.008.

[41] F.A. Leibfarth, K.M. Mattson, B.P. Fors, H.A. Collins, C.J. Hawker, External regulation of controlled polymerizations, Angew. Chemie Int. Ed. 52 (1) (2013) 199–210, https://doi.org/10.1002/anie.201206476.

[42] Z. Nie, E. Kumacheva, Patterning surfaces with functional polymers, Nat. Mater. 7 (4) (2008) 277–290, https://doi.org/10.1038/nmat2109.

[43] Mingxiao Li, Michele Fromel, Dhanesh Ranaweera, Sergio Rocha, Cyrille Boyer, Christian W. Pester, SI-PET-RAFT: surface-initiated photoinduced electron transfer-reversible addition-fragmentation chain transfer polymerization, ACS Macro Lett. 8 (4) (2019) 374–380, https://doi.org/10.1021/acsmacrolett.9b0008910.1021/acsmacrolett.9b00089.s001.

[44] W. Sheng, B. Li, X. Wang, B. Dai, B. Yu, X. Jia, F. Zhou, Brushing up from "anywhere" under sunlight: a universal surface-initiated polymerization from polydopamine-coated surfaces, Chem. Sci. 6 (3) (2015) 2068–2073, https://doi.org/10.1039/c4sc03851g.

[45] J. Yan, B. Li, F. Zhou, W. Liu, Ultraviolet light-induced surface-initiated atom-transfer radical polymerization, ACS Macro Lett. 2 (7) (2013) 592–596, https://doi.org/10.1021/mz400237w.

[46] Y. Nakayama, T. Matsuda, Surface macromolecular architectural designs using photo-graft copolymerization based on photochemistry of benzyl N, N-Diethyldithiocarbamate, Macromolecules 29 (27) (1996) 8622–8630, https://doi.org/10.1021/ma9606014.

[47] Michele Fromel, Mingxiao Li, Christian W. Pester, Surface engineering with polymer brush photolithography, Macromol. Rapid Commun. 41 (18) (2020) 2000177, https://doi.org/10.1002/marc.v41.1810.1002/marc.202000177.

[48] C.M. Weber, C.N. Berglund, P. Gabella, Mask cost and profitability in photomask manufacturing: an empirical analysis, IEEE Trans. Semicond. Manuf. 19 (4) (2006) 465–474, https://doi.org/10.1109/TSM.2006.883577.

[49] C.W. Pester, B. Narupai, K.M. Mattson, D.P. Bothman, D. Klinger, K.W. Lee, E. H. Discekici, C.J. Hawker, Engineering surfaces through sequential stop-flow photopatterning, Adv. Mater. 28 (42) (2016) 9292–9300, https://doi.org/10.1002/adma.201602900.

[50] Alexa M. Wong, Daniel J. Valles, Carlos Carbonell, Courtney L. Chambers, Angelica Y. Rozenfeld, Rawan W. Aldasooky, Adam B. Braunschweig, Controlled-height brush polymer patterns via surface-initiated thiol-methacrylate photopolymerizations, ACS Macro Lett. 8 (11) (2019) 1474–1478, https://doi.org/10.1021/acsmacrolett.9b0069910.1021/acsmacrolett.9b00699.s001.

[51] C. Carbonell, D. Valles, A.M. Wong, A.S. Carlini, M.A. Touve, J. Korpanty, N. C. Gianneschi, A.B. Braunschweig, Polymer brush hypersurface photolithography, Nat. Commun. 11 (1) (2020) 1244, https://doi.org/10.1038/s41467-020-14990-x.

[52] Q. Geng, D. Wang, P. Chen, S.C. Chen, Ultrafast multi-focus 3-D nano-fabrication based on two-photon polymerization, Nat. Commun. 10 (1) (2019) 1–7, https://doi.org/10.1038/s41467-019-10249-2.

[53] K. Itoga, J. Kobayashi, M. Yamato, T. Okano, Micropatterning with a Liquid Crystal Display (LCD) projector, Methods Cell Biol. 119 (2014) 141–158, https://doi.org/10.1016/B978-0-12-416742-1.00008-1.

[54] S. Shanmugam, J. Xu, C. Boyer, Exploiting metalloporphyrins for selective living radical polymerization tunable over visible wavelengths, J. Am. Chem. Soc. 137 (28) (2015) 9174–9185, https://doi.org/10.1021/jacs.5b05274.

[55] N. Mataga, Y. Shibata, H. Chosrowjan, N. Yoshida, A. Osuka, Internal conversion and vibronic relaxation from higher excited electronic state of porphyrins: femtosecond fluorescence dynamics studies, J. Phys. Chem. B 104 (17) (2000) 4003–4004, https://doi.org/10.1021/jp9941256.

[56] G.G. Gurzadyan, T.H. Tran-Thi, T. Gustavsson, Time-resolved fluorescence spectroscopy of high-lying electronic states of Zn-tetraphenylporphyrin, J. Chem. Phys. 108 (2) (1998) 385–388, https://doi.org/10.1063/1.475398.

[57] Wenqing Yan, Sajjad Dadashi-Silab, Krzysztof Matyjaszewski, Nicholas D. Spencer, Edmondo M. Benetti, Surface-initiated photoinduced ATRP: mechanism, oxygen tolerance, and temporal control during the synthesis of polymer brushes, Macromolecules 53 (8) (2020) 2801–2810, https://doi.org/10.1021/acs.macromol.0c0033310.1021/acs.macromol.0c00333.s001.

[58] B. Narupai, Z.A. Page, N.J. Treat, A.J. McGrath, C.W. Pester, E.H. Discekici, N. D. Dolinski, G.F. Meyers, J. Read de Alaniz, C.J. Hawker, Simultaneous preparation of multiple polymer brushes under ambient conditions using microliter volumes, Angew. Chemie Int. Ed. 57 (41) (2018) 13433–13438, https://doi.org/10.1002/anie.201805534.

[59] T. Zhang, Y. Du, J. Kalbacova, R. Schubel, R.D. Rodriguez, T. Chen, D.R.T. Zahn, R. Jordan, Wafer-scale synthesis of defined polymer brushes under ambient conditions, Polym. Chem. 6 (47) (2015) 8176–8183, https://doi.org/10.1039/c5py01274k.

[60] Nathaniel Corrigan, Dzulfadhli Rosli, Jesse Warren Jeffery Jones, Jiangtao Xu, Cyrille Boyer, Oxygen tolerance in living radical polymerization: investigation of mechanism and implementation in continuous flow polymerization, Macromolecules 49 (18) (2016) 6779–6789, https://doi.org/10.1021/acs.macromol.6b0130610.1021/acs.macromol.6b01306.s001.

[61] Matthew D. Ryan, Ryan M. Pearson, Tracy A. French, Garret M. Miyake, Impact of light intensity on control in photoinduced organocatalyzed atom transfer radical polymerization, Macromolecules 50 (12) (2017) 4616–4622, https://doi.org/10.1021/acs.macromol.7b0050210.1021/acs.macromol.7b00502.s001.

[62] Mingxiao Li, Michele Fromel, Dhanesh Ranaweera, Christian W. Pester, Comparison of long-term stability of initiating monolayers in surface-initiated controlled radical polymerizations, Macromol. Rapid Commun. 41 (17) (2020) 2000337, https://doi.org/10.1002/marc.v41.1710.1002/marc.202000337.